Bimodal Expression of the *Salmonella* Typhimurium *spv* Operon

Ioannis Passaris,[1] Alexander Cambré, Sander K. Govers,[2] and Abram Aertsen[3]
Department of Microbial and Molecular Systems (M²S), Katholieke Universiteit Leuven, 3001 Leuven, Belgium
ORCID IDs: 0000-0003-0260-4054 (S.K.G.); 0000-0002-1897-2305 (A.A.)

ABSTRACT The well-studied *spv* operon of *Salmonella typhimurium* is important for causing full virulence in mice and both the regulation and function of the Spv proteins have been characterized extensively over the past several decades. Using quantitative single-cell fluorescence microscopy, we demonstrate the *spv* regulon to display a bimodal expression pattern that originates in the bimodal expression of the SpvR activator. The *spv* expression pattern is influenced by growth conditions and the specific *S. typhimurium* strain used, but does not require *Salmonella*-specific virulence regulators. By monitoring real-time promoter kinetics, we reveal that SpvA has the ability to impart negative feedback on *spvABCD* expression without affecting *spvR* expression. Together, our data suggest that the SpvA protein counteracts the positive feedback loop imposed by SpvR, and could thus be responsible for dampening *spvABCD* expression and coordinating virulence protein production in time. The results presented here yield new insights in the intriguing regulation of the *spv* operon and adds this operon to the growing list of virulence factors exhibiting marked expression heterogeneity in *S. typhimurium*.

KEYWORDS bimodality; *Salmonella typhimurium*; *spv* operon; *spvA*

SALMONELLA species comprise important Gram-negative intestinal pathogens with the capacity to survive and multiply intracellularly in various mammals and, depending on the serovar, can cause two major clinical syndromes in humans: typhoid fever, which is a systemic and potentially fatal invasive disease affecting multiple organs in the body, and nontyphoid gastroenteritis, which causes a usually self-limiting diarrheal disease (Coburn *et al.* 2007; McQuiston *et al.* 2008; Fabrega and Vila 2013). The serovar *Salmonella typhimurium* is commonly isolated in gastroenteritis disease outbreaks and harbors a wide range of virulence factors that are typically located on laterally acquired genetic elements such as *Salmonella* pathogenicity islands (SPIs) (large genomic regions containing multiple virulence factors) and virulence plasmids (Rhen and Dorman 2005; Hébrard *et al.* 2011; Sterzenbach *et al.* 2013).

As such, SPI-1 is the best characterized pathogenicity island and is mainly important for the intestinal phase of *S. typhimurium* infection (Lee *et al.* 1992; Mills *et al.* 1995; Phoebe Lostroh and Lee 2001). The genes on this island encode several effector proteins that are secreted through a type three secretion system (TTSS) (termed TTSS-1 and encoded within SPI-1) into the intestinal epithelial cells to facilitate invasion and subsequent internalization of *Salmonella* (Rhen and Dorman 2005; Morgan 2007). The SPI-2 island of *S. typhimurium* encodes its own secretion system (TTSS-2), and different effectors facilitating survival and replication inside epithelial cells and macrophages (Hensel *et al.* 1995; Ochman *et al.* 1996; Figueira and Holden 2012). Regulation of gene expression from both islands is extremely complex and involves a network of interacting transcriptional regulators that are responsive to a combination of environmental and intracellular signals (Deiwick *et al.* 1999; Worley *et al.* 2000; Brown *et al.* 2005; Bustamante *et al.* 2008; Fass and Groisman 2009; Saini *et al.* 2010; Sturm *et al.* 2011).

S. typhimurium also harbors the pSLT virulence plasmid of ~90 kb that contains a highly conserved ca. 8 kb region of

doi: https://doi.org/10.1534/genetics.118.300822
Manuscript received February 13, 2018; accepted for publication August 14, 2018; published Early Online August 16, 2018.
Supplemental material available at Figshare: https://doi.org/10.25386/genetics.6976106.
[1]Present address: Department of Biology, Centre for Immunology and Infection, University of York, York YO10 5DD, United Kingdom.
[2]Present address: Jacobs-Wagner Lab, Microbial Sciences Institute, Department of Molecular, Cellular and Developmental Biology, Yale University, New Haven, Connecticut 06516.
[3]Corresponding author: Department of Microbial and Molecular Systems (M²S), Katholieke Universiteit Leuven, Kasteelpark Arenberg 22, 3001 Leuven, Belgium. E-mail: abram.aertsen@kuleuven.be

five genes (*spvRABCD*) that have been reported to be implicated in intracellular survival and growth (Gulig and Doyle 1993; Libby *et al.* 1997; Cano *et al.* 2001) and killing of (mostly) macrophages (Guilloteau *et al.* 1996; Libby *et al.* 2000). The SpvB, SpvC, and SpvD proteins have unequivocally been proven to be virulence factors with specific roles in infected host cells (Tezcan-Merdol *et al.* 2005; Browne *et al.* 2008; Mazurkiewicz *et al.* 2008; Haneda *et al.* 2012; Rolhion *et al.* 2016) and are thought to be exported outside the cell mainly through the TTSS-2 (Browne *et al.* 2002; Gotoh *et al.* 2003; Mazurkiewicz *et al.* 2008). In particular, SpvB has been characterized as an (ADP-ribosyl)transferase, activating host cell actin degradation and thereby mediating cytotoxicity in macrophages and virulence in mice (Mazurkiewicz *et al.* 2008), while SpvC was found to exhibit phosphothreonine lyase activity on host mitogen-activated protein kinases (MAPKs), leading to attenuation of the intestinal inflammatory response, which is thought to be important during systemic infection of *S. typhimurium* (Otto *et al.* 2000). Recently, the function and crystal structure of the SpvD protein were elucidated and it was found that SpvD acts as a cysteine protease, which downregulates proinflammatory responses by indirectly inhibiting NF-κB regulated promoters and by doing so contributes to the systemic growth of *S. typhimurium* in mice (Grabe *et al.* 2016; Rolhion *et al.* 2016). In contrast, little is known about the SpvA protein and it is yet unclear if it is involved in *Salmonella* virulence (Roudier *et al.* 1992; Rotger and Casadesus 1999). While many global regulators can influence *spv* expression (Fang *et al.* 1992; Kowarz *et al.* 1994; O'Byrne and Dorman 1994a,b; Robbe-Saule *et al.* 1997; Marshall *et al.* 1999; Mangan *et al.* 2006), the *spvR* gene that is located directly upstream of the *spvABCD* operon is thought to be transcribed separately (Robbe-Saule *et al.* 1997; Wilson and Gulig 1998) and encodes the DNA-binding SpvR protein, which acts as an essential activator of both *spvR* and the *spvABCD* genes and is absolutely required for *spv*-mediated virulence *in vivo* (Grob and Guiney 1996; Guilloteau *et al.* 1996; Sheehan and Dorman 1998).

Apart from the timely expression of virulence factors, *Salmonella* appears to exploit population heterogeneity as an important aspect of its virulence as well (Stewart and Cookson 2012; Ackermann 2015). In fact, *Salmonella* benefits from the creation of phenotypically heterogeneous subpopulations to enable bet-hedging and division-of-labor strategies that are indispensable for proper colonization of its host and for the survival in nonhost environments (Ackermann *et al.* 2008; Arnoldini *et al.* 2014; MacKenzie *et al.* 2015). Most notably in this context, the regulatory architecture of the SPI-1 gene circuit results in the bistable expression of the SPI-1 genes that gives rise to a subpopulation of SPI-1–expressing cells that produce the costly TTSS-1 components to invade the gut tissue and elicit gut inflammation, and of cells that do not express SPI-1 and manage to outcompete the gastrointestinal microbiota by respiring inflammation specific compounds (Hautefort *et al.* 2003; Saini *et al.* 2010; Sturm *et al.* 2011; Diard *et al.* 2013; Bäumler and Sperandio 2016). As opposed to SPI-1 expression, the expression pattern of the SPI-2 genes does not exhibit a clear bifurcation in ON and OFF cells, but rather corresponds to an inducible expression pattern where the whole population turns on SPI-2 gene expression when making the transition from extracellular to intracellular environments (Hautefort *et al.* 2003; Laughlin *et al.* 2014).

In this study, we used random transposition of a promoterless *yfp* gene (encoding the yellow fluorescent protein) to examine single-cell level gene expression from the *S. typhimurium* pSLT plasmid and found that the *spv* operon exhibits a bimodal expression pattern with only a subset of the population actively expressing the *spv* genes. We confirmed the indispensable role of SpvR in *spv* expression and extended its function with respect to the bimodal expression of the *spvABCD* genes. Moreover, we identified the SpvA protein as an important regulator of *spv* expression and provide evidence that SpvA is necessary in obtaining coordinated *spvR* and *spvABCD* expression.

Materials and Methods

Strains and growth conditions

Bacterial strains, phages, and plasmids used throughout this study are listed in Supplemental Material, Tables S1 and S2. *S. typhimurium* LT2 was used for transposon mutagenesis of pSLT and the more virulent *S. typhimurium* ATCC14028s strain was used for all subsequent experiments involving *spv* regulation. For culturing bacteria, lysogeny broth (LB; Sambrook and Russell 2001) medium was standardly used either as broth or as agar plates after the addition of 1.5% (for spreading plates) or 0.7% (for soft-agar plates) agar. Cultures were grown in LB broth for 16–20 hr at 37° under well-aerated conditions (200 rpm on an orbital shaker) to reach stationary phase. Exponential phase cultures were in turn prepared by diluting stationary phase cultures 1/100 or 1/1000 in prewarmed broth, and allowing further incubation at 37° until an optical density at 630 nm (OD = 630) of 0.4–0.6 was reached. In indicated cases, intracellular salts medium (ISM) (Headley and Payne 1990), containing 1% glycerol as a carbon source and with a pH of 6, was used. Finally, the transposon mutagenesis screen was performed using AB minimal medium supplemented with 0.2% glucose as a carbon source (Clark and Maaløe 1967) (http://openwetware.org/wiki/AB_medium).

When appropriate, the following chemicals (Applichem, Darmstadt, Germany) were added to the growth medium at the indicated final concentrations: ampicillin (100 μg/ml; Ap^{100}), chloramphenicol (30 μg/ml; Cm^{30}), kanamycin (50 μg/ml; Km^{50}), tetracycline (20 μg/ml; Tc^{20}), anhydrotetracycline (aTc; different concentrations), and L-arabinose (0.2%).

Phages were propagated on S. *typhimurium* LT2 or ATCC14028s as plaques in LB soft-agar or as lysates in LB broth as described previously (Davis *et al.* 1980). Phage stocks were filter sterilized with 0.2 μm filters (Thermo Fisher Scientific, Aalst, Belgium) and chloroform was added to maintain

sterility. Generalized transduction was performed with phage P22 *HT105/1 int-201* as described previously (Schmieger 1972; Davis *et al.* 1980). This mutant is unable to integrate into the host chromosome as a prophage due to the lack of integrase activity.

Construction of the Tn5-mVenus transposon

The Tn*5-mVenus* transposon was largely designed *in silico* and obtained from a DNA synthesis company (GenScript). For its use, the Tn*5-mVenus* transposon was cut out of its cloning vector (pUC57) using the *Pvu*II restriction enzyme and ligated bluntly in the backbone of the pBAM1-GFP plasmid (Martínez-García *et al.* 2011). The pBAM1-GFP plasmid had been cut as well with *Pvu*II (thereby removing its *gfp* gene) and the backbone was extracted from an agarose gel using the GeneJet Gel Extraction Kit (Thermo Fisher Scientific). The ligation mix was electroporated to an *Escherichia coli* S17-1λ*pir* strain and Ap^R colonies were PCR verified for the integration of the Tn*5-mVenus* transposon and subsequently sequenced.

Next, a sequence verified clone was used to incorporate a neomycin phosphotransferase (*npt*) cassette, conferring Km^R, and a PCR-based strategy was followed. The pBAM1-Tn*5-mVenus* backbone was amplified using an outward PCR, with primers containing 5′ *Bam*HI restriction enzyme sites and subsequently cut with *Bam*HI. In parallel, the *npt* cassette was PCR amplified from the pKD4 plasmid (Datsenko and Wanner 2000) using primers with a 5′ *Bam*HI restriction enzyme site, and cut with *Bam*HI. This fragment was used for sticky end ligation in the *Bam*HI-treated pBAM1-Tn*5-mVenus* PCR fragment and the ligation mixture was electroporated to *E. coli* S17-1λ*pir*, selecting on Km^R. Resistant colonies were picked up and sequence verified. The complete sequence of this transposon can be provided upon request.

Transposon mutagenesis of pSLT using Tn5-mVenus and screening

Suicide delivery of the Tn*5-mVenus* transposon was accomplished through mating of donor and acceptor strains (Martínez-García *et al.* 2011). More specifically, the donor (*E. coli* S17-1λ*pir* strain bearing the pBAM1-Tn*5-mVenus* plasmid) and the acceptor (*S. typhimurium* LT2 *finO*::*TetRA*) were grown overnight with the appropriate antibiotics. Deletion of the pSLT-borne *finO* gene increases conjugation efficiency (Camacho and Casadesus 2002) and was necessary to avoid enrichment of pSLT *finO* mutants in the second conjugation step. Next, cells were washed with 10 mM $MgSO_4$ and four times concentrated. Then, 100 μl of donor and 100 μl of acceptor were thoroughly mixed in 5 ml of 10 mM $MgSO_4$ and further concentrated onto a filter disk (0.45 μm pore, 47 mm diameter; Pall). The filter was subsequently incubated on an LB agar plate for 2–4 hr at 30°, after which it was transferred to 5 ml of a 10 mM $MgSO_4$ solution and intensely vortexed to resuspend the cells. Finally, cells were plated out on AB minimal medium plates containing kanamycin to counterselect for the donor strain in mating. The occurrence of plasmid integrants, instead of the desired transposon mutants, was checked through streaking out on Ap^{100} (backbone marker of pBAM1), and it was found that mutant libraries contained 1–10% false positives. This value is acceptable due to the large sizes of the constructed libraries. The specificity for pSLT mutants was accomplished through a second conjugation step. The constructed library of ~13,000 Tn*5-mVenus* mutants was pooled together and used as a donor library in a mating with the *S. typhimurium* LT2 *mrr*::*Cm* Δ*pSLT* recipient strain, after which the mixture was plated on AB minimal medium containing kanamycin and chloramphenicol. Using this protocol, chromosomal transposon insertions present in the donor library were efficiently separated from the insertions in pSLT that could be collected in the final recipient. The latter collection was subsequently used for screening for fluorescent mutants.

The mutant library was screened using both fluorescence microscopy and fluorescence-activated cell sorting (FACS). In the first approach, 1720 mutants were manually screened using fluorescence microscopy and the retrieved fluorescent mutants were stored at −80°. An alternative approach was adopted where the remaining pSLT mutants were pooled together and subjected to one round of FACS to enrich for mVenus-expressing mutants. These mutants were validated using fluorescence microscopy and stored at −80°. Finally, all transposon insertions yielding fluorescent mutants were transferred to clean background strains using generalized transduction and their insertion location was determined.

Mapping of transposon insertions

Mapping of the transposon insertions was performed in analogy with the method used by Kwon and Ricke (2000). First, 20 μl of linker1 (350 ng/μl) (Table S3) was added to 18 μl of phosphorylated linker2 (350 ng/μl) and heated for 2 min at 95°, after which the mixture was left to cool down and allow annealing of the linkers (Y-linker). Genomic DNA of transposon mutants was extracted via phenol:chloroform extraction (Wilson 2001) and completely digested with *Nla*III (Thermo Fisher Scientific). The digested DNA was purified with the GeneJet PCR Purification kit (Thermo Fisher Scientific) and ~40 μg was ligated to 1 μg of the Y-linker with 1 μl of T4 DNA ligase (1 unit/μl; Thermo Fisher Scientific) in a final volume of 20 μl. After overnight incubation at 22° the reaction mixture was heated at 65° for 10 min to denature the ligase. A total of 2 μl of this mixture was used as DNA template in a PCR mixture together with a primer specific to the transposon (Tn5-mVenus_up_out), a primer specific to the Y-linker (Y-linker primer) and a Taq polymerase (DreamTaq DNA polymerase; Thermo Fisher Scientific). The PCR products were purified, sequenced (EZ-seq; Macrogen, Amsterdam, The Netherlands) and the exact position of the transposon was determined using a basic local alignment search tool (BLAST). In the *spvA*::Tn*5-mVenus* mutant the transposon was inserted 177 bp downstream of the +1 transcription start site, while in the *spvB*::Tn*5-mVenus* mutant, the transposon was inserted 1047 bp downstream of the transcription start site.

Construction of bacterial mutants

All *S. typhimurium* mutants were constructed via a λ-red–mediated homologous recombination approach (Datsenko and Wanner 2000). The temperature-sensitive pKD46 plasmid was routinely used to provide the λ-red genes under arabinose inducible control and strains containing the plasmid were typically grown to exponential phase at 30°, whereupon arabinose was added for an extra 30 min. Subsequently the cells were made electrocompetent, by keeping them at 4° and washing them three times with Milli-Q water, and the PCR product was electroporated, after which the cells were left to resuscitate for a couple of hours at 37°. Cells were plated out at 37° (to cure them from pKD46) on LB medium complemented with an appropriate antibiotic to select for recombinants, and validated through PCR with primer pairs flanking the homologous region. Correct integration of PCR products was further verified by sequencing (EZ-seq; Macrogen). All primer sequences for constructing the bacterial mutants with a detailed description are listed in Table S3. The antibiotic cassette was usually flanked by *frt* sites and could thus be flipped out by providing cells with the site-specific Flp recombinase (Cherepanov and Wackernagel 1995). Cells were first electroporated with the temperature-sensitive pCP20 plasmid, constitutively expressing the Flp recombinase, and flipping was verified using PCR and sequencing. The pCP20 plasmid was cured by growing the strains at 37° and loss of pCP20 was verified by streaking the cells on Ap^{100} -containing medium. All strains containing multiple fluorescence markers were constructed through sequential recombination steps and all the different loci targeted in the final strain were PCR-validated and sequence-verified. The *rpoS* deletion was first constructed in a *S. typhimurium* ATCC14028s background using λ-red–mediated homologous recombination, and subsequently introduced in the relevant *spvA* reporter strains using generalized transduction with P22 *HT105/1 int-201*.

The pSLT-*spvA*::Tn*5-mVenus* plasmid was transferred from *Salmonella* to *E. coli* MG1655 *cat-lacI* via conjugation and conjugants were selected on LB medium containing both Cm^{30} (to counter-select the donor strain) and Km^{50}.

FACS, time-lapse fluorescence microscopy, and image analysis

The pooled pSLT::Tn*5-mVenus* library was sorted by a FACS (BD influx cell sorter) to enrich for mVenus-expressing mutants. A 488 nm excitation laser in combination with a 530/40 nm emission filter was used, and the ±0.1% most mVenus fluorescent clones were sorted and plated out on AB minimal medium containing Km^{50}.

Fluorescence microscopy was further used to screen for fluorescent transposon mutagenesis mutants. All fluorescence microscopy and time-lapse fluorescence microscopy experiments were performed with a temperature-controlled (Okolab, Ottaviano, Italy), Ti-Eclipse inverted microscope (Nikon, Champigny-sur-Marne, France) equipped with a TI-CT-E motorized condenser, a YFP filter (Ex 500/24 nm, DM 520 nm, Em 542/27 nm), a DAPI filter (Ex 377/50 nm, DM 409 nm, Em 447/60), a GFP filter (Ex 473/30, Dm 495, Em 520/35), an mCherry filter (Ex 562/40, Dm 593, Em 647/75), and a CoolSnap HQ2 FireWire CCD-camera.

For imaging, cells were grown to midlog or stationary phase and placed between LB or ISM agarose pads and a cover glass, essentially as described previously (Cenens *et al.* 2013), and incubated at 37°. Images were acquired using NIS-Elements (Nikon) and resulting pictures were further handled with open-source software ImageJ (downloaded from http://rsbweb.nih.gov/ij/). Detailed image analysis was performed using the open source MicrobeTracker software (Sliusarenko *et al.* 2011) and the cell meshes generated by this software were used to measure the average cellular fluorescence. The average cellular fluorescence was determined by dividing the integrated pixel intensities of individual cells (after background subtraction) by their respective areas. Appropriate bins for the average cellular fluorescence were chosen by visual inspection of *spv* ON and *spv* OFF cells. In short, for every experiment, a threshold was set to separate ON cells from OFF cells and this was based on inspecting single-cell fluorescence intensities in the image and visually defining them as ON or OFF.

Data availability

Strains and plasmids are available upon request. File S1 contains supplemental figures and tables. File M1 contains Movie 1. File M2 contains Movie 2. Supplemental material available at Figshare: https://doi.org/10.25386/genetics.6976106.

Results

The spvABCD operon is expressed in a bimodal fashion

A random transposon mutagenesis approach using a modified Tn*5* transposon (termed Tn*5-mVenus* and encoding the YFP variant mVenus; Figure 1A) was used to specifically target the pSLT virulence plasmid of *S. typhimurium* LT2 in an effort to better characterize its encoded functions. The Tn*5-mVenus* transposon has the potential of creating C-terminal mVenus translational fusions when randomly inserted into a gene in the correct orientation and reading frame, thereby allowing one to visualize protein expression and/or localization patterns using fluorescence microscopy. During our screening procedure, two transposon mutants were picked up that showed marked expression heterogeneity, with only a small subpopulation of cells actively expressing the mVenus protein (termed ON cells throughout the manuscript) compared to a majority of nonfluorescent siblings (OFF cells) (Figure 1, C and D). Interestingly, the transposon insertions could be mapped to the *spvA* (*i.e.*, the *spvA*::Tn*5-mVenus* mutant, yielding the SpvA_59::mVenus C-terminal protein fusion) and *spvB* (*i.e.*, the *spvB*::Tn*5-mVenus* mutant, yielding the SpvB_349::mVenus C-terminal protein fusion) genes, which are part of the well-studied pSLT-borne *spvABCD* virulence

operon (Figure 1B). Although both the function and the regulation of the *spv* genes has been studied extensively over the past 25 years, this is, to the best of our knowledge, the first time these genes are being reported to have a bimodal expression pattern.

Since the *S. typhimurium* LT2 strain is known to be virulence attenuated (Wilmes-Riesenberg *et al.* 1997), the transposon insertions were transduced to the *S. typhimurium* ATCC14028s strain, which has retained its lethality in mice and its ability to survive in murine macrophages (Jarvik *et al.* 2010). Comparison of the frequency of *spvA* ON cells in *S. typhimurium* LT2 and *S. typhimurium* ATCC14028s revealed a significant difference between both strains of respectively 3.2% *spvA* ON cells *vs.* 7.3% *spvA* ON cells (Figure 2A and Figure S1A, i and ii) in LB medium. In addition to the difference in frequency, the fluorescence intensity of *spvA* ON cells (measured as the average cellular fluorescence, described in the *Materials and Methods* section) in *S. typhimurium* LT2 was also lower than that in *S. typhimurium* ATCC14028s (Figure S1A, v; white and light gray bars). *S. typhimurium* LT2 has been shown to have decreased RpoS protein levels due to a rare UUG start codon in the *rpoS* gene (Wilmes-Riesenberg *et al.* 1997), and the *spv* operon has been shown to be regulated by RpoS (Norel *et al.* 1992; Kowarz *et al.* 1994). To address if RpoS has an influence on the frequency of *spvA* ON cells, the *rpoS* allele was knocked out in both the LT2 and ATCC14028s *spvA*::Tn*5-mVenus* strains. It was found that knocking out *rpoS* completely abrogated *spvA* expression for both strains in LB (Figure S2), suggesting that different RpoS levels between LT2 and ATCC14028s might be influencing the frequency of *spvA* ON cells. Since these observations indicate that proper *spv* expression is better studied in the *S. typhimurium* ATCC14028s strain, all strains mentioned throughout the rest of this article were constructed in this background.

It has previously been described that *spvABCD* expression is more pronounced in ISM, which mimics the intracellular environment of mammalian cells and has been used routinely to study *spv* regulation (Wilson *et al.* 1997; Wilson and Gulig 1998). Indeed, when a population of the *S. typhimurium* ATCC14028s *spvA*::Tn*5-mVenus* transposon mutant was grown to stationary phase in ISM, the frequency of *spvA* ON cells significantly increased when compared to LB medium (28.2% *spvA* ON cells *vs.* 7.3% *spvA* ON cells, respectively; Figure 2, one-way ANOVA followed by Tukey's honest significant difference test was performed on the whole data set to compare the mean percentage of *spvA* ON cells of each strain in both media and statistical significance was found for every strain on the $P < 0.01$ significance level), although the ON cells showed on average a higher fluorescence signal when originating in LB medium (Figure S1, A and B, v). The outcome of the *spv* bimodal response thus strongly depends on environmental inputs.

To ensure that the bimodal response of the transposon mutants was not an artifact of the transposon mutagenesis or screening protocol, an *S. typhimurium* ATCC14028s reporter strain was *de novo* constructed in which the mVenus fluorescent protein was translationally fused C-terminally to the SpvA protein (*spvA*::*mVenus*). The resulting strain was grown in both LB and ISM and monitored under the microscope, and again a clear bimodal expression pattern could be observed (Figure S1, A and B, iv), confirming the phenotype observed with our transposon insertion mutants. It was noticed, however, that the fluorescence intensity of the *spvA* signal (Figure S1, A and B, v) and the proportion of *spvA* ON cells (Figure 2) was considerably lower in the *S. typhimurium* ATCC14028s *spvA*::*mVenus* strain when compared to the *S. typhimurium* ATCC14028s *spvA*::Tn*5-mVenus* transposon mutant (respectively, 3.9% *vs.* 7.3% *spvA* ON cells in LB and 21.6% *vs.* 28.2% spvA ON cells in ISM), and this observation is further elaborated upon below.

Next, we translationally fused the mCherry fluorescent protein to the C-terminus of SpvC in the *S. typhimurium* ATCC14028s *spvB*::Tn*5-mVenus* strain and observed a bimodal expression pattern for SpvC (Figure S3A). Furthermore, all *spvC* ON cells were also *spvB* ON, suggesting that the entire *spvABCD* operon is simultaneously expressed in a bimodal fashion.

The pSLT plasmid can be conjugated to *E. coli* as well (Ahmer *et al.* 1999), and upon conjugating the *spvA*::Tn*5-mVenus* encoding pSLT plasmid to *E. coli* K-12 MG1655, it was observed that *spvA* expression in this background was also bimodal and that both burst frequency and intensity compared very well to *Salmonella* burst frequency and intensity (Figure 1C and Figure S3, B and C). This latter observation suggests that bimodality of the *spv* operon is insulated from the regulation imposed by *Salmonella*-specific virulence regulators.

SpvR determines the frequency of spvA ON cells and is itself expressed in a bimodal fashion

Since SpvR constitutes the essential activator protein of the *spvABCD* operon, we aimed to examine its effect on the observed bimodality as well. In this regard, a *S. typhimurium* ATCC14028s strain was constructed in which the *spvR* promoter was replaced by the synthetic $P_{LtetO\text{-}1}$ promoter (Lutz and Bujard 1997), resulting in aTc-inducible expression of *spvR*, and the *msfGFP* gene was inserted transcriptionally directly downstream of the 3′ end of *spvA*. Using this strain ($P_{LtetO\text{-}1}$-*spvR_spvA-msfGFP*), a clear range of aTc concentrations could be distinguished, yielding populations with only *spvA* OFF cells (<2 ng/ml aTc), a bimodal regime with both *spvA* ON and OFF cells (2–8 ng/ml aTc), and finally populations with only *spvA* ON cells (>8 ng/ml aTc) (Figure 3). In the bimodal regime, the proportion of *spvA* ON cells increased from ca. 40% at 2 ng/ml aTc to ca. 90% at 4 ng/ml aTc and reaching ca. 99% at 8 ng/ml aTc, and the average cellular fluorescence intensity of the *spvA* ON cells increased accordingly (Figure 3B). Together, this confirms the essential role of SpvR in *spvA* expression and further shows that a certain threshold concentration of SpvR should be reached to fully induce *spvA* expression, and when SpvR concentrations

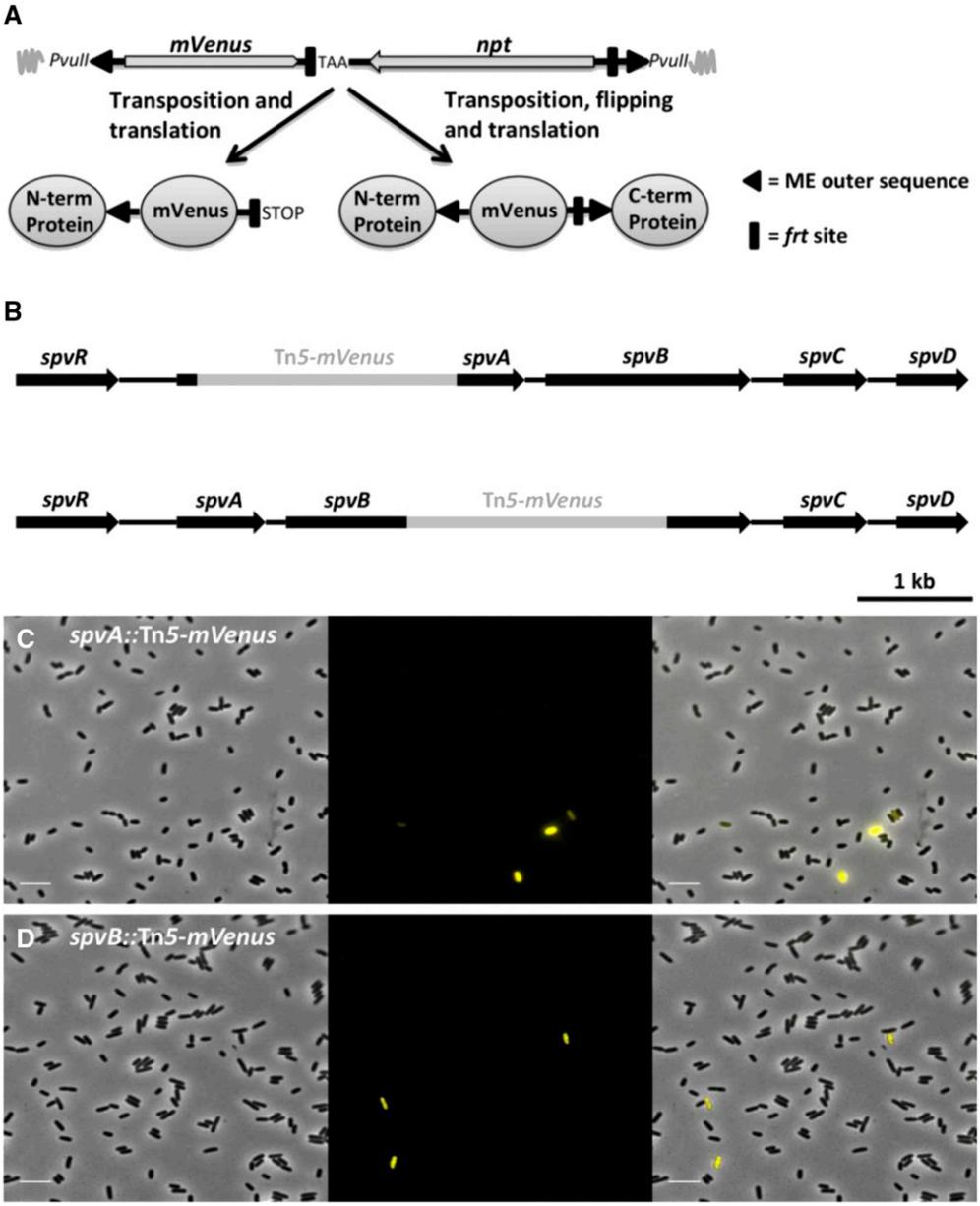

Figure 1 Bimodal expression of *spvA* and *spvB* in *S. typhimurium* LT2. (A) Schematic of the constructed Tn*5-mVenus* transposon (total size of 2248 bp) as integrated in the pBAM1 plasmid and the different fluorescent protein fusions it is able to generate after in frame transposition. The *mVenus* gene lacks its natural stop codon but a stop codon has been incorporated right after the left *frt* site. The *Pvu*II restriction enzyme sites were used for cloning the transposon in the pBAM1 plasmid. Image not drawn to scale. (B) Schematic showing the exact insertion position of the Tn*5-mVenus* transposon into the *spvA* gene, yielding the SpvA_59::mVenus C-terminal fusion protein (top scheme), and *spvB* gene, yielding the SpvB_349::mVenus C-terminal fusion protein (bottom scheme). (C) Representative image of the *spvA*::Tn*5-mVenus* mutant yielding the SpvA_59::mVenus C-terminal protein grown to stationary phase in AB minimal medium. (D) Representative image of the *spvB*::Tn*5-mVenus* mutant yielding the SpvB_349::mVenus C-terminal protein fusion grown to stationary phase in AB minimal medium. The pixel intensities in the different frames are not comparable and the images are merely a qualitative illustration of the bimodal expression of *spvA* and *spvB*. The image panels represent the phase contrast channel, the YFP fluorescent channel, and the two channels merged. Bar, 5 μm.

fluctuate around this threshold, the population can bifurcate into an *spvA* ON and *spvA* OFF population.

Moreover, these data suggest that the origin of the bimodal expression pattern of *spvA* lies in the expression of *spvR*. To test whether *spvR* is also expressed in a bimodal fashion and overlaps with *spvA* expression, a new *S. typhimurium* ATCC14028s strain was constructed in which the *msfGFP* gene was transcriptionally inserted directly downstream of the *spvR* gene, while the *mCherry* gene was transcriptionally inserted directly downstream of the *spvA* gene (*spvR-msfGFP_spvA-mCherry*). Expression of *spvR* was indeed found to be bimodal, and the msfGFP and mCherry signal exhibited a strong positive correlation with two distinct clusters representing the *spv* OFF and ON populations ($R^2 = 0.9375$; Figure 4, A and C), suggesting that *spvR* and *spvA* expression levels are highly interlinked with each other. Furthermore, when monitoring this strain with time-lapse microscopy, it could be observed that P_{spvR} and P_{spvA} bursting were correlated in time as well (Figure 5). Together, the results presented in this section suggest that bimodality of the *spvABCD* operon is causally preceded by the bimodal expression of SpvR.

Deletion of spvA increases its own promoter activity without affecting spvR expression

When comparing the fluorescence signal from the *spvA*::Tn*5-mVenus* allele (in which mVenus is preceded by the first 59 amino acids of SpvA) to the *de novo* constructed *spvA*::*mVenus* allele (in which mVenus is preceded by the full length of SpvA), it was observed that the latter allele caused a decreased amount of *spvA* ON cells and that these *spvA* ON cells exhibited a reduced fluorescence intensity, both in LB and ISM (Figure 2 and Figure S1, A and B, v). Furthermore,

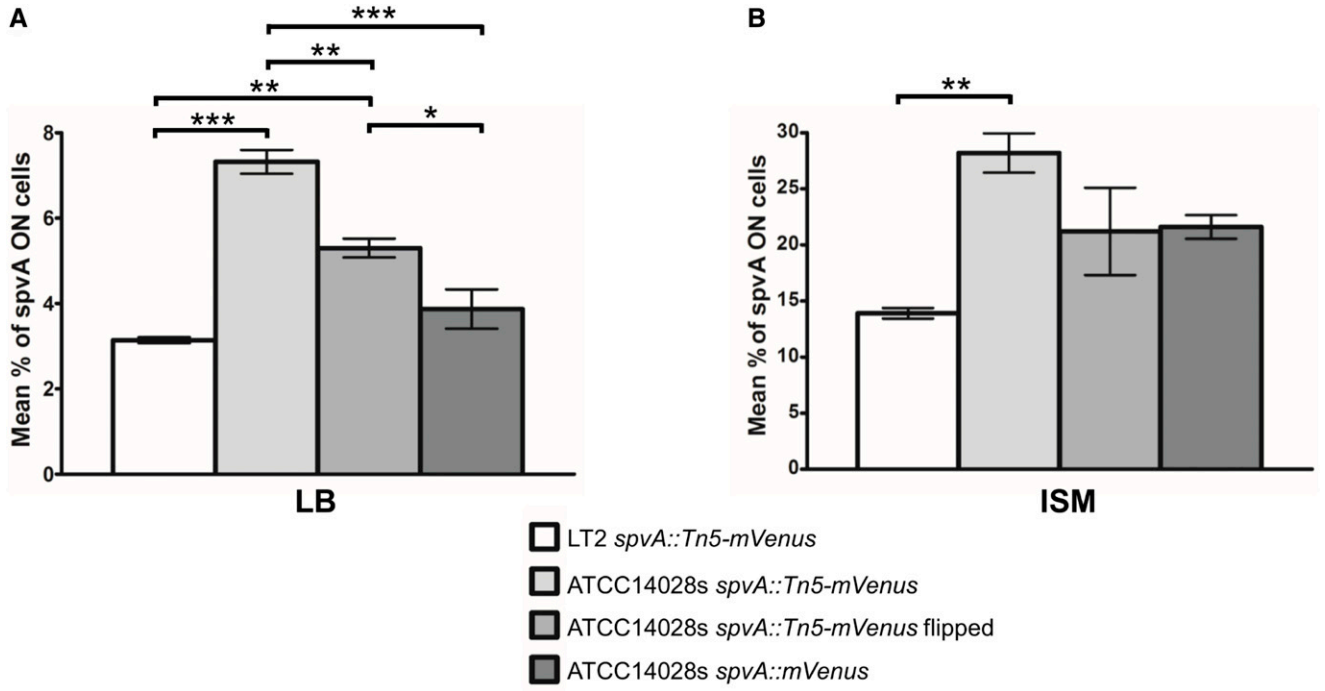

Figure 2 The proportion of *spvA* ON cells in populations of the indicated strains grown to stationary phase in LB (A) or ISM (B). Cells of the corresponding populations were analyzed with fluorescence microscopy and binned as ON when their mVenus fluorescence exceeded 10 A.U., with this cut-off being based on visual inspection of the raw microscopy images. The data show the mean proportion of *spvA* ON cells in the total population with the corresponding SEM from three biological replicates. The number of cells quantified for every biological replicate of each strain in both growth media was in the range of 800–2200 cells. One-way ANOVA, followed by Tukey's honest significant difference test, was performed on the two separate data sets to test for statistically significant differences between the strains (* $P < 0.05$, ** $P < 0.01$, *** $P < 0.001$).

when flipping out the *npt* cassette in the *spvA*::Tn*5-mVenus* mutant (Figure S1), yielding a strain expressing the SpvA_59::mVenus::SpvA_197 "sandwich" fusion protein (where the mVenus protein is now followed by the remaining 197 C-terminal amino acids of SpvA), again a decreased number of *spvA* ON cells (Figure 2) with a substantially lower fluorescence intensity compared to the parental *spvA*::Tn*5-mVenus* mutant was observed, more closely matching the intensities of the *spvA*::*mVenus* allele (Figure S1, v). Together, these preliminary observations suggested that completely abrogating the SpvA protein leads to an increase in *spvA* expression.

To independently confirm the above observations, a clean knockout strain of *spvA* was constructed *de novo* in the *S. typhimurium* ATCC14028s *spvR-msfGFP* background where only the first 10 amino acids of SpvA were kept and translationally fused to the mCherry fluorescent protein (Δ*spvA*::*mCherry*). The fluorescence intensity of the ON cells in the *spvR-msfGFP_*Δ*spvA*::*mCherry* strain was subsequently compared to the *spvR-msfGFP_spvA-mCherry* strain and it was observed that the *spv* ON cells in the Δ*spvA* strain showed a substantially higher mCherry fluorescence intensity compared to the *spv* ON cells in the strain containing a functional *spvA* copy (Figure 4, A and B). Quantification of the average cellular fluorescence intensity of both strains revealed that the proportion of P_{spvA} ON cells (*i.e.*, the mCherry signal) was higher in the *spvR-msfGFP_*Δ*spvA*::*mCherry* strain (38.6% ON cells for *spvR-msfGFP_spvA-mCherry* strain *vs.* 45.8% for the *spvR-msfGFP_*Δ*spvA*::*mCherry* strain), and that the average cellular fluorescence intensity of the P_{spvA} ON cells in the Δ*spvA* strain was substantially higher giving rise to a well-separated, highly fluorescent subpopulation (Figure 4, B, D, and F).

Quantification of the average cellular msfGFP fluorescence of both strains did not show any marked difference in both the proportion of P_{spvR} ON cells or the average cellular msfGFP fluorescence intensity between the two strains (42.0% ON cells for *spvR-msfGFP_spvA-mCherry* strain *vs.* 42.9% ON cells for the *spvR-msfGFP_*Δ*spvA*::*mCherry* strain; Figure 4E) and suggests that the increased expression from P_{spvA} in the Δ*spvA*::*mCherry* strain is not caused by an increased expression of the SpvR activator. In addition to this, the msfGFP and mCherry signals are still highly positively correlated ($R^2 = 0.7993$; Figure 4D) in the *spvR-msfGFP_*Δ*spvA*::*mCherry* strain, indicating that P_{spvR} and P_{spvA} expression are still intimately coupled. However, when comparing Figure 4, C and D it is clear that the *spvR-msfGFP_*Δ*spvA*::*mCherry* strain reaches higher P_{spvA} expression levels compared to the *spvR-msfGFP_spvA-mCherry* strain and this for similar P_{spvR} expression levels.

Together, these data confirm that functionally compromising the SpvA protein leads to an increase in *spvA* promoter activity. At the same time, these results also suggest that the increased expression driven from the *spvA* promoter is not

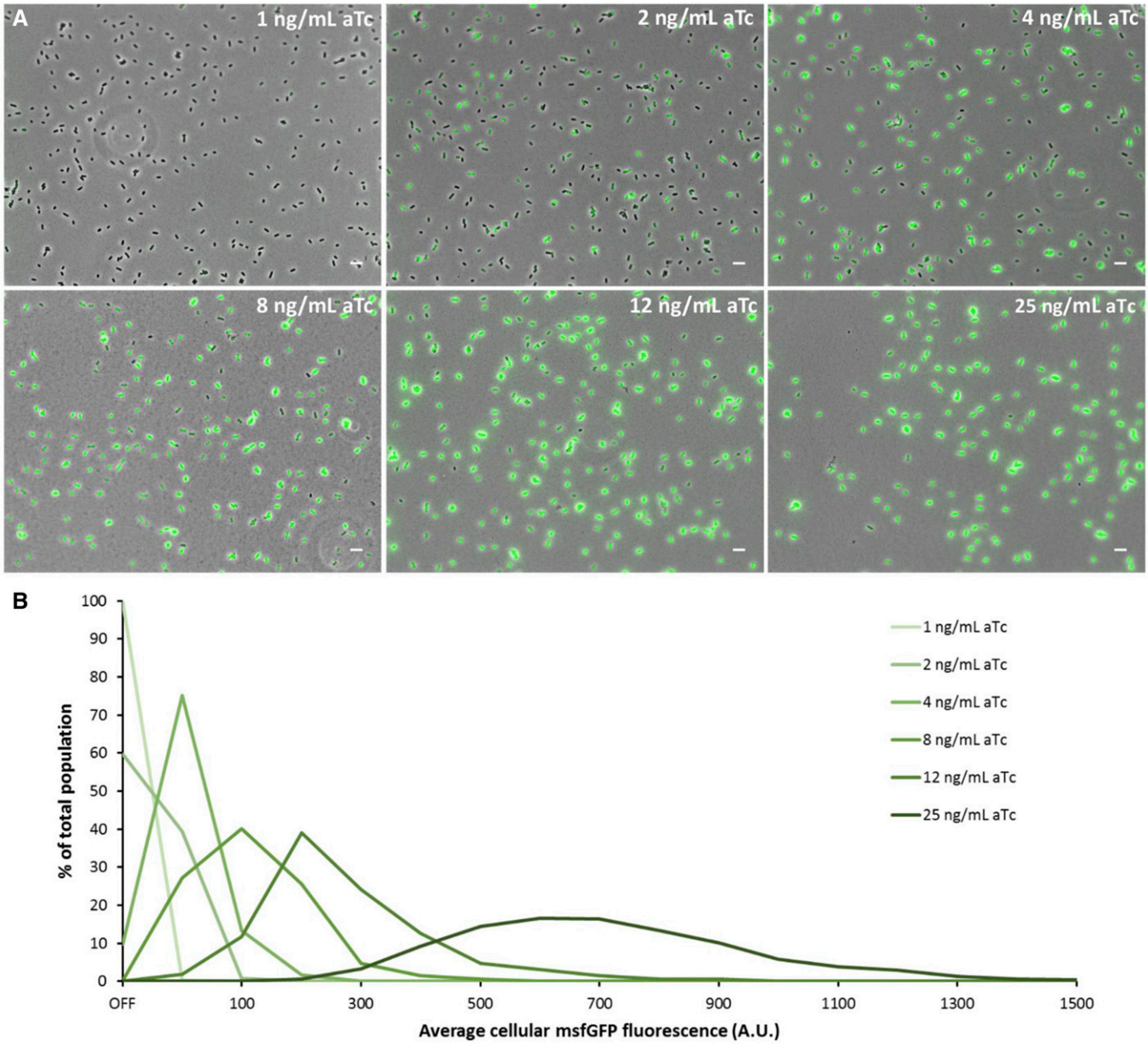

Figure 3 SpvR determines the proportion of *spvA* ON cells and the intensity of *spvA* expression. (A) Representative images (overlay of phase contrast and GFP channels) of the *S. typhimurium* ATCC14028s $P_{LtetO\text{-}1}$-*spvR_spvA-msfGFP* strain grown overnight in ISM containing 1 ng/ml aTc, 2 ng/ml aTc, 4 ng/ml aTc, 8 ng/ml aTc, 12 ng/ml aTc, and 25 ng/ml aTc. (B) Histogram (based on the experiment shown in A) displaying the distribution of the average cellular fluorescence intensity for the different aTc concentrations. The OFF bin in this experiment was set between 0 and 10 A.U., based on visual inspection of the raw microscopy images. The first ON bin was between 10 and 50 A.U. and subsequent bins were defined every 50 A.U. The number of cells (*n*) used for quantification was as follows: *n* = 2050 (1 ng/ml aTc), *n* = 1678 (2 ng/ml aTc), *n* = 1751 (4 ng/ml aTc), *n* = 1726 (8 ng/ml aTc), *n* = 1871 (12 ng/ml aTc), and *n* = 1615 (25 ng/ml aTc). The experiment was repeated on several independent occasions and similar trends were observed. The pixel intensities of the images in A are not directly comparable with each other and the images are merely a qualitative illustration of the differently sized subpopulations observed. The image panels in A represent the phase contrast channel merged with the GFP fluorescent channel. Bar, 5 μm.

directly caused by an increased *spvR* expression, which complicates the interpretation of the Δ*spvA* phenotype.

Deletion of spvA reveals uncoordinated P_{spvA} and P_{spvR} bursting

To investigate the role of SpvA in altering *spvA* and *spvR* expression in more detail, time-lapse fluorescence microscopy was performed on the *spvR-msfGFP_ΔspvA::mCherry* strain to better characterize the coordination between P_{spvR} and P_{spvA} bursting behavior in time. Interestingly, in this strain, P_{spvR} and P_{spvA} bursting appeared not as tightly coordinated and predictable as in the *spvR-msfGFP_spvA::mCherry* strain, and different bursting characteristics could be discriminated (Figure 5 *vs.* Figure 6 and Figure S4). While the scenario in which P_{spvR} bursting is quickly followed by P_{spvA} bursting was still observed (Figure 6, purple arrows),

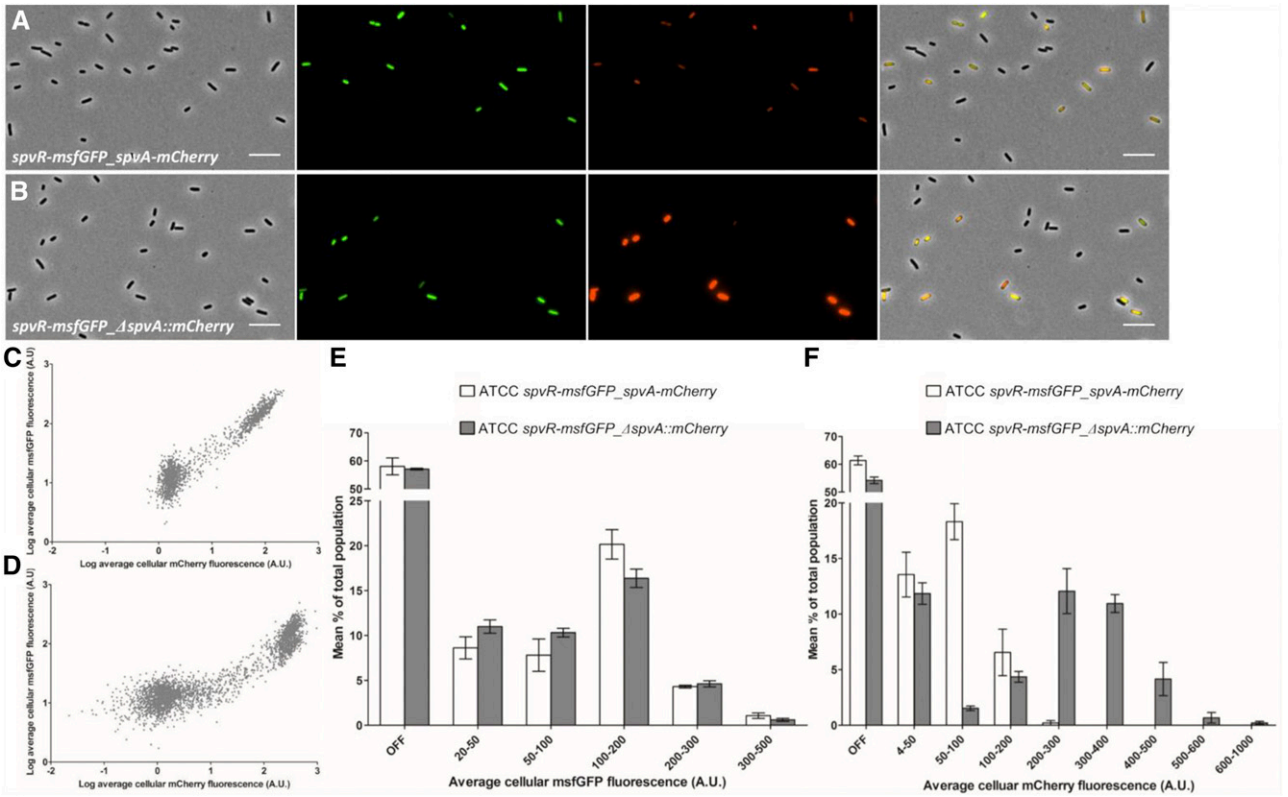

Figure 4 Expression of *spvR* and *spvA* is highly correlated. (A) Representative image of the *S. typhimurium* ATCC14028s *spvR-msfGFP_spvA-mCherry* strain grown to stationary phase in ISM. (B) Representative image of the *S. typhimurium* ATCC14028s *spvR-msfGFP_ΔspvA::mCherry* strain grown to stationary phase in ISM. The pixel intensities in A and B have been adjusted similarly for the msfGFP and mCherry channel to make them visually comparable. The image panels in A and B represent the phase contrast channel, the GFP fluorescent channel, the mCherry fluorescent channel, and the three channels merged. Bar, 5 μm. (C) Scatterplot showing the average cellular mCherry and msfGFP fluorescence of all three biological replicates of the *spvR-msfGFP_spvA-mCherry* strain. (D) Scatterplot showing the average cellular mCherry and msfGFP fluorescence of all three biological replicates of the *spvR-msfGFP_ΔspvA::mCherry* strain. (E) Histogram showing the distribution of the average cellular msfGFP fluorescence within populations of the *spvR-msfGFP_spvA-mCherry* (open bars) and *spvR-msfGFP_ΔspvA::mCherry* (shaded bars) strains. Averages and the corresponding SEM from three biological replicates are shown. (F) Histogram showing the distribution of average the cellular mCherry fluorescence within populations of the *spvR-msfGFP_spvA-mCherry* (open bars) and *spvR-msfGFP_ΔspvA::mCherry* (shaded bars) strains. Averages and the corresponding SEM from three biological replicates are shown. The OFF bin was set between 0 and 20 A.U. (E) and 0–4 A.U. (F), and was based on visual inspection of the raw microscopy images. The number of cells quantified for every biological replicate of every strain was in the range of 560–1130 cells.

in more than half of the bursting cells, P_{spvA} bursting occurred without an observable P_{spvR} burst preceding it (Figure 6 and Figure S4, white arrows). In those cases, P_{spvR} bursting could usually be observed somewhat later in P_{spvA} ON cells and, interestingly, this P_{spvR} burst seemed necessary to sustain the initial P_{spvA} burst and to fully induce both genes over time (Figure 6 and Figure S4, blue and yellow arrows). As mentioned previously, if no SpvR protein is present, no *spvA* expression could be observed (Figure 3A) and this might imply that our microscopy set-up is not sensitive enough to detect (smaller) *spvR* bursts possibly occurring below our camera's detection limit.

To further reveal the effect of the SpvA protein on its own expression while trying to minimize potential polar effects in the fluorescent reporter strains, an alternative approach was pursued based on *ssrA*-mediated tagging of the SpvA and/or msfGFP protein (Andersen *et al.* 1998). Specific tagging of the C terminus of these proteins with an 11 amino acid *ssrA* tag (the last three amino acids determine the degradation rate and were LAA in this study) makes them recognizable for intracellular tail-specific proteases, leading to their rapid degradation and thus the possibility to monitor real-time promoter bursting more accurately.

In this regard, a new reporter strain was constructed to assert real-time P_{spvA} bursting. This was achieved through insertion of the *msfGFP* gene, containing its own ribosome binding site, start codon, and a C-terminal *ssrA* degradation tag, right after the 3′ end of the *spvA* gene (*i.e.*, the *spvA-msfGFP-LAA* strain) (Figure 7A). When monitoring this strain (expressing wild-type SpvA) using time-lapse fluorescence microscopy, short-lived bursting events were observed but only in a limited number of cells (Figure 7A and File M1, Movie 1). Next, we reasoned that if the SpvA protein itself would be actively degraded as well, thus mimicking a functional knockdown of SpvA, then different bursting kinetics should be observed. To test this, a strain was constructed in which, in addition to the *msfGFP-LAA* part, the *ssrA* degradation tag was also fused directly to the C terminus of the SpvA

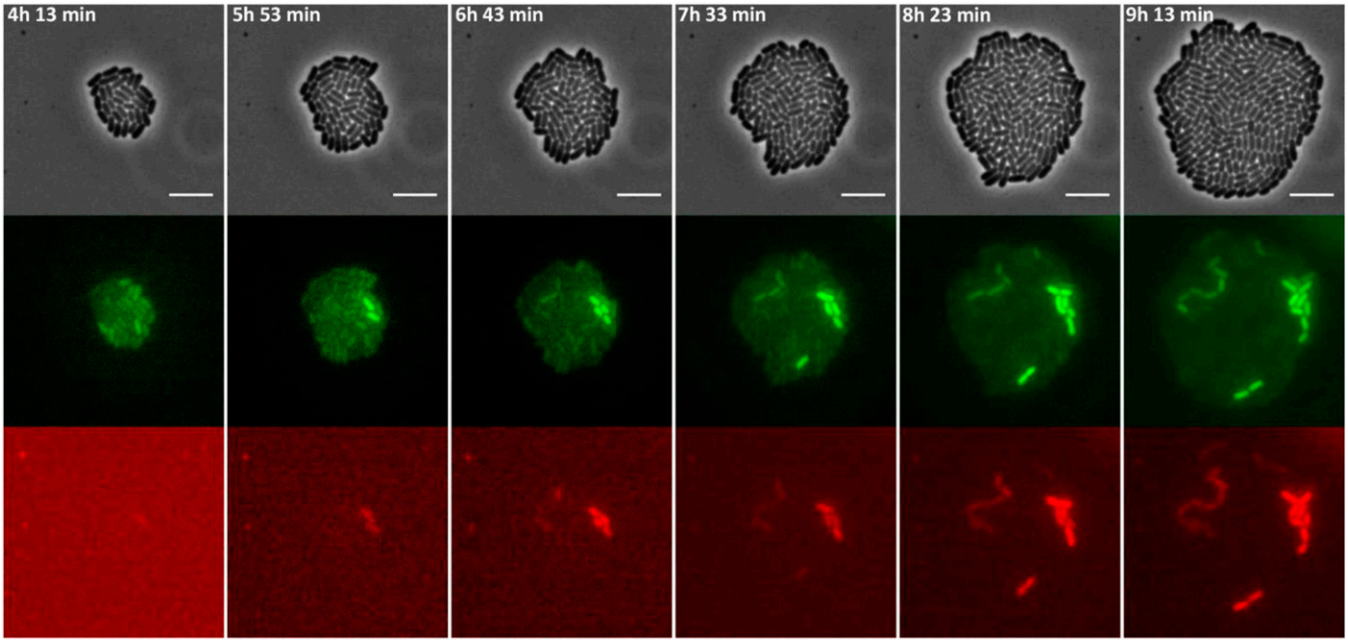

Figure 5 Images of a time-lapse fluorescence microscopy recording of the growth of a representative microcolony of the *S. typhimurium* ATCC14028s *spvR-msfGFP_spvA-mCherry* strain showing highly coordinated P_{spvR} and P_{spvA} bursting. The strain was grown to stationary phase in ISM and subsequently monitored on ISM agarose pads at 37° for the time indicated. The pixel intensities in the different frames are not comparable and the images are merely a qualitative illustration of the bursting process. The image panels represent the phase contrast channel, the GFP fluorescent channel, and the mCherry fluorescent channel. Bar, 5 μm.

protein (*i.e.*, the *spvA-LAA-msfGFP-LAA* strain), yielding a strain where the SpvA protein is prone to degradation (Figure 7B). Interestingly, when performing time-lapse fluorescence microscopy with this strain and comparing with the *spvA-msfGFP-LAA* strain, it was observed that bursting events appeared more pronounced, with more cells showing bursting behavior, bursting cells exhibiting higher but more variable burst sizes, and bursting events being sustained for a longer time period (Figure 7B and File M2, Movie 2). The latter was quantified in more detail and it was found that the average burst time of *spvA-msfGFP-LAA* cells was 56 min, while the average burst time increased significantly to 218 min in *spvA-LAA-msfGFP-LAA* cells (Figure 7C and Figure S5).

Together, these results clearly underscore the ability of the SpvA protein to impart regulatory feedback on the *spv* operon, although further research is required to determine the underlying molecular mechanism and possible contributions of potential polar effects in the engineered reporter strains.

Discussion

The *spv* operon is an important and conserved virulence trait in most *Salmonella enterica* strains (with *S. typhi*, *S. paratyphi*, and *S. sendai* being important exceptions) and has been shown to be important for triggering and maintaining systemic disease in mice, and required for causing nontyphoid extraintestinal disease with bacteremia in humans (Rotger and Casadesus 1999; Guiney and Fierer 2011). While the regulation of this operon has been studied extensively over the past several decades, the bimodal expression pattern of these genes has not been reported. Moreover, the single-cell data reported here were derived from strains in which the *spv* genes are kept in their native genomic context, and this implies that previous work on *spv* expression, based on population-level assays and often the use of multicopy plasmids, should be interpreted with care and with the concepts of burst frequency (*i.e.*, the number of *spv* ON cells in the population), burst intensity (*i.e.*, the intensity of *spv* expression), and burst time (*i.e.*, the duration of being ON) in mind.

Time-lapse fluorescence microscopy analysis revealed that P_{spvR} and P_{spvA} bursting are perfectly coordinated, and that P_{spvR} bursting precedes and is responsible for subsequent P_{spvA} bursting. The observed heterogeneity appears to be supported by the genetic architecture of the *spv* regulon, which seems to fulfill some key features known to be important for bimodal expression patterns. First of all, the fact that the SpvR protein is an activator of its own expression, thus creating a positive feedback loop, is a hallmark for bimodal expression systems (Ferrell 2002). In addition to this positive feedback loop, the system should display nonlinear kinetics, which in the case of the *spv* operon is likely accomplished through dimerization of the SpvR protein and subsequent binding on P_{spvR} and P_{spvA}, and cooperative binding of SpvR dimers to two distinct operators site of P_{spvA} (termed the promoter proximal site and the promoter distal site), further amplifying the nonlinear kinetics of this promoter (Grob and Guiney 1996; Sheehan and Dorman 1998). As a result, in cells stochastically expressing a higher number of SpvR

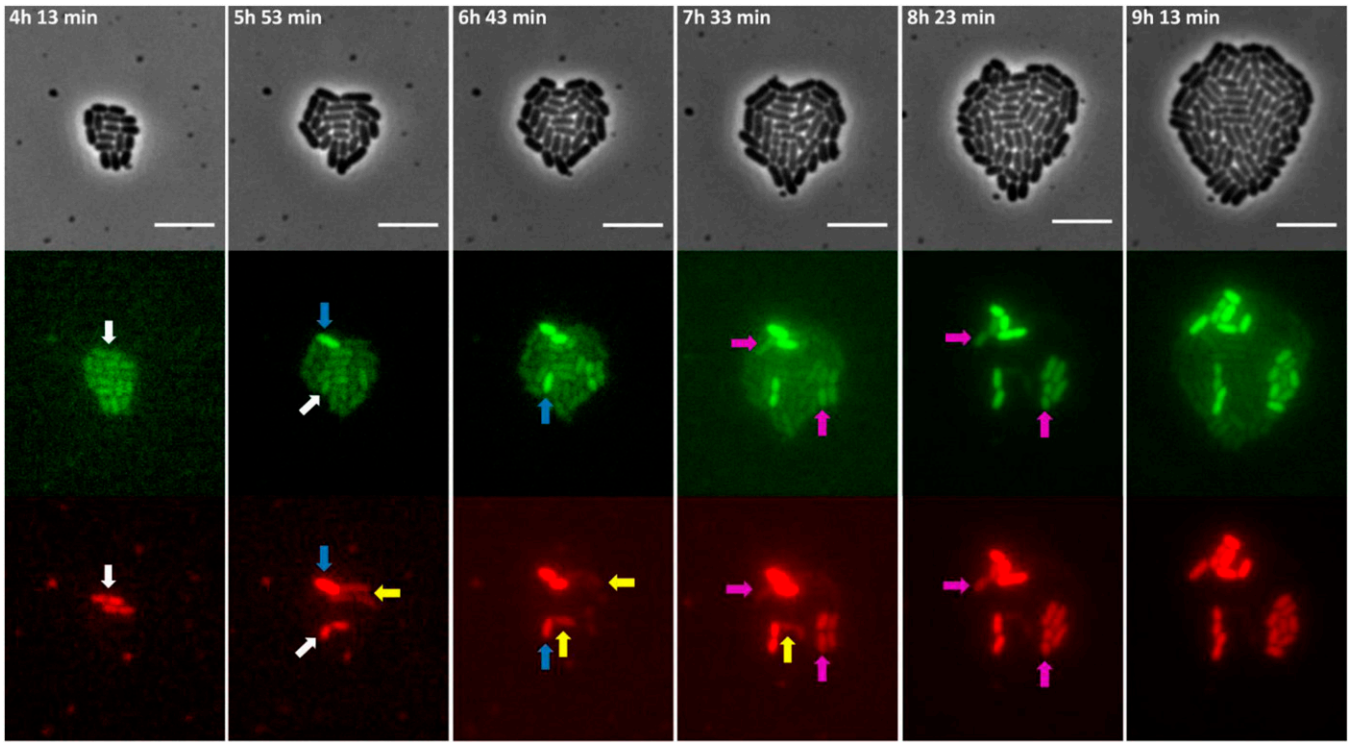

Figure 6 Images of a time-lapse fluorescence microscopy recording of the growth of a representative microcolony of the *S. typhimurium* ATCC14028s *spvR-msfGFP_ΔspvA::mCherry* strain showing heterogeneous and uncoordinated P_{spvR} and P_{spvA} bursting. The strain was grown to stationary phase in ISM and subsequently seeded and monitored on ISM agarose pads at 37° for the time indicated. White arrows indicate cells with an initial P_{spvA} burst but without an observable P_{spvR} burst. Blue arrows indicate cells with a delayed observable P_{spvR} burst leading to a sustained P_{spvA} burst. Yellow arrows indicate cells in which the initial P_{spvA} burst is not sustained in time, likely due to lack of an observable P_{spvR} burst. Purple arrows indicate cells in which P_{spvA} and P_{spvR} bursting is coordinated, reminiscent of the dynamics of the *S. typhimurium* ATCC14028s *spvR-msfGFP_spvA::mCherry* strain. The pixel intensities in the different frames are not comparable and the images are merely a qualitative illustration of the bursting process. The image panels represent the phase contrast channel, the GFP fluorescent channel and the mCherry fluorescent channel. Bar, 5 μm.

molecules, SpvR would be more prone to bind the *spvR* (establishing the positive feedback loop) and *spvA* promoter, thereby activating *spv* expression. So far, it has been shown that the *spvR* locus contains one dominant promoter with only one SpvR operator site and a putative translational enhancer element within the 5′ *spvR* coding sequence (Sheehan and Dorman 1998; Robbe-Saule *et al.* 1999), and future work should address whether *spvR* bimodality can be attributed solely to these elements or if an (unknown) upstream factor is required as well. In the later context, the observation that the proportion of *spv* ON cells increases in ISM when compared to LB medium suggests the presence of an extra signal facilitating SpvR in engaging the positive feedback loop, and the existence of such a signal has already been postulated in earlier studies (Robbe-Saule *et al.* 1997; Wilson *et al.* 1997; Sheehan and Dorman 1998).

Importantly, when looking at the real-time P_{spvA} bursting events in single cells, short-lived promoter bursts were observed and it seems unlikely that these would be able to sustain a stable *spv* ON state for multiple generations. The *spv* genetic circuit thus seems to resemble an excitable system rather than a pure bistable system. In short, excitable systems are known to exhibit an activation pulse after a certain threshold crossing event and are generally driven by positive and negative feedback loops with different time scales (Süel *et al.* 2006; Eldar and Elowitz 2010; Young *et al.* 2013; Martins and Locke 2015). Furthermore, the activation pulse causes a transient drift away from the rest state in which the system is temporarily insensitive to further input, but does not fix the system in two stable states, as is the case for bistable systems.

Interestingly, we observed that compromising SpvA function increased the expression directed from P_{spvA}, suggesting that the SpvA protein establishes a negative feedback loop acting on the *spvA* promoter. The increase in *spvA* promoter activity is not due to an increased *spvR* expression and shows that the *spvR* and *spvA* promoters, although intimately linked, seem to be uncoupled to a certain extent. This finding seems to contradict other studies where SpvA has been shown to repress *spvR* expression (Spink *et al.* 1994; Abe and Kawahara 1995; Wilson and Gulig 1998). In this regard, it should be noted that these studies were performed on the population level (using northern blots, immunoblots, and β-galactosidase assays), and often using multicopy plasmids, which might have skewed these observations. Time-lapse fluorescence microscopy further showed that in an *spvA* compromised strain, the timing and coordination of P_{spvR}-P_{spvA} bursting was altered, giving rise to a less coordinated, less predictable, and more

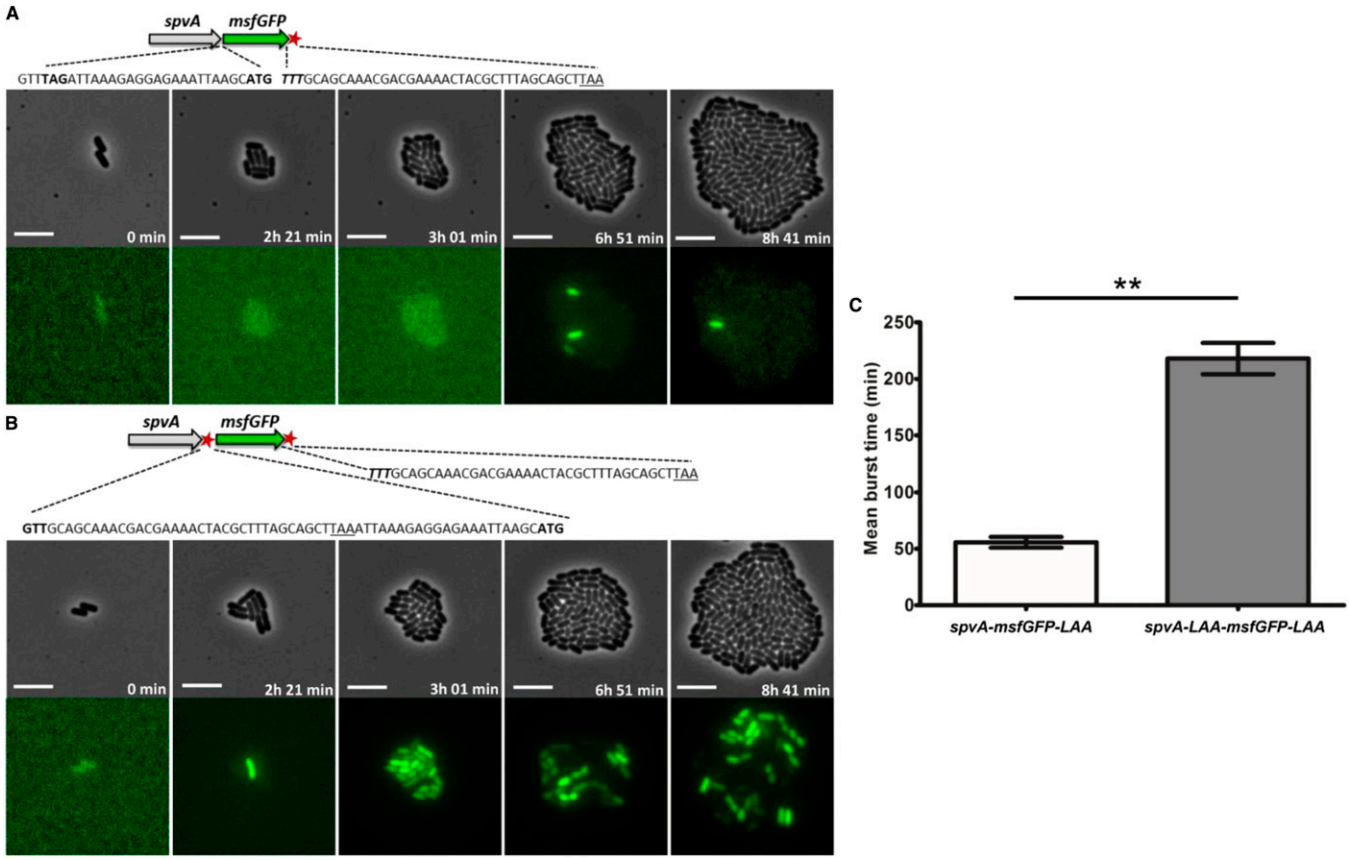

Figure 7 Images of a time-lapse fluorescence microscopy recording of the growth of a representative microcolony of the (A) *S. typhimurium* ATCC14028s *spvA-msfGFP-LAA* and the (B) *S. typhimurium* ATCC14028s *spvA-LAA-msfGFP-LAA* strain, showing different P_{spvA} bursting dynamics. (A) Schematic of the *S. typhimurium* ATCC14028s *spvA-msfGFP-LAA* strain with the *ssrA* tag shown as a red asterisk. The junction site between *spvA* and *msfGFP* is shown in more detail with the TAG stop codon of SpvA (shown in bold), followed by the ribosome biding site (RBS) and ATG start codon of *msfGFP* (shown in bold). The 3′ end of *msfGFP* constitutes of the penultimate TTT codon of *msfGFP* (shown in bold and in italics), followed by the *ssrA* degradation tag sequence, and a TAA stop codon (underlined). (B) Schematic of the *S. typhimurium* ATCC14028s *spvA-LAA-msfGFP-LAA* strain with the *ssrA* tags shown as red asterisks. The junction site between *spvA* and *msfGFP* is shown in more detail with the penultimate GTT codon of SpvA (shown in bold) followed by the *ssrA* degradation tag sequence, a TAA stop codon (underlined), and the RBS and ATG start codon of *msfGFP* (shown in bold). The 3′ end of *msfGFP* is identical to the one described in A. (C) Mean burst times of the *spvA-msfGFP-LAA* strain and the *spvA-LAA-msfGFP-LAA* strain. The burst time was defined as the time in which an individual cell showed an msfGFP signal that exceeded the background levels of OFF cells until this signal faded and returned to background levels again. The mean burst times and SEM for two biological replicates are shown and an unpaired *t*-test was performed to test for statistical significance (** $P < 0.01$). The strains were grown to stationary phase in ISM and subsequently seeded and monitored on ISM agarose pads at 37° for the time indicated. The pixel intensities between A and B, and in the different frames, are not comparable and the images are merely a qualitative illustration of the bursting process. The image panels represent the phase contrast channel and the GFP fluorescent channel. Bar, 5 μm.

heterogeneous bursting process. Real-time P_{spvA} bursting in a strain actively degrading the SpvA protein seems to support the latter statement. In this strain bursting cells are abundant and show very pronounced bursting behavior with higher burst sizes and with longer lasting bursts, when compared with the strain having an intact SpvA protein. Although potentiating polar effects in the engineered reporter strains cannot be excluded, the SpvA protein seems to have the ability to control P_{spvA} bursting behavior through a negative feedback loop, counteracting the positive feedback loop SpvR imposes, and so contributes to the excitability of the *spv* system. It is likely that the SpvR-mediated positive feedback loop and the SpvA-mediated negative feedback loop are indeed working on different time scales, with the positive feedback loop setting in first and leading to expression of the *spvABCD* operon, after which the SpvA-mediated negative feedback loop kicks in and quickly curbs *spvABCD* expression. This creates a situation where a subset of cells highly expresses the SpvABCD virulence proteins, and only for a limited amount of time.

It currently remains unclear whether the (potentially bet-hedging) bifurcation in a heterogeneous *spv* ON and *spv* OFF population is the actual biological aim of the *spv* regulon, or rather a side-effect of its genetic wiring. In fact, the SpvR-mediated positive feedback loop could also be viewed as a kind of memory function that is needed to sustain a short activation pulse for a time period lasting longer than the actual activation pulse (as is typically the case for excitable

systems which, after a threshold crossing event, are insensitive to further input; Martins and Locke 2015). This implies that the *spv* operon would always be induced in the niche where all of its inducing agents are present (presumably inside the macrophage) and that the genetic architecture has evolved in a way to provide the right amount of virulence protein for the right amount of time (even when the initial inducing signals are not present anymore). Bifurcation of the population in *spv* ON and OFF negative cells would then rather be a side-effect of inappropriate or insufficient inducing conditions where *spvR* activation is occurring on a purely stochastic base.

It is yet unclear how SpvA would exert this negative feedback loop, but considering the fact that the protein does not contain any predicted DNA binding domains and has previously been shown to reside in the outer membrane (although it lacks any typical N-terminal secretion signals) (Valone and Chikami 1991; El-Gedaily *et al.* 1997), it seems that we can rule out a direct effect on the *spvA* promoter. More work is needed to further confirm this regulatory feedback, to precisely map the domain(s) responsible for SpvA-mediated repression and to find out how this outer membrane protein exactly causes these changes in *spvABCD* gene expression. We speculate that other factors are involved and act together with SpvA in tuning the bimodal response of the *spv* genes, but further research is needed to fully characterize this intricate genetic circuit on the singe-cell level.

The bimodal expression pattern of the *spv* regulon is another addition to *Salmonella*'s realm of heterogeneously expressed virulence operons and future work should address how this pattern is integrated into the sophisticated infection strategies of these notorious pathogens.

Acknowledgments

The authors would like to thank William Cenens, Peter Goos, Kristof Vanoirbeek, Catherine Royer, and Marjan van der Woude for helpful suggestions and fruitful discussions; Sander Van Dromme for helping to screen the Tn*5-mVenus* mutant library; Víctor de Lorenzo for his kind gift of the pBAM1-GFP plasmid; and Johan Paulsson for his kind gift of the pDHL1029 plasmid. This work was supported by doctoral fellowships from the Flemish Agency for Innovation by Science and Technology (IWT-Vlaanderen; to I.P. and S.K. G.) and the Research Foundation - Flanders (FWO-Vlaanderen; to A.C.), and a grant from the Katholieke Universiteit Leuven Research Fund (IDO/10/012). The funders had no role in study design, data collection and analysis, decision to publish, or preparation of the manuscript. The authors declare no conflicts of interest.

Literature Cited

Abe, A., and K. Kawahara, 1995 Transcriptional regulation and promoter sequence of the *spvR* gene of virulence plasmid pKDSC50 in *Salmonella choleraesuis* serovar Choleraesuis. FEMS Microbiol. Lett. 129: 225–230.

Ackermann, M., 2015 A functional perspective on phenotypic heterogeneity in microorganisms. Nat. Rev. Microbiol. 13: 497–508. https://doi.org/10.1038/nrmicro3491

Ackermann, M., B. Stecher, N. E. Freed, P. Songhet, W. D. Hardt *et al.*, 2008 Self-destructive cooperation mediated by phenotypic noise. Nature 454: 987–990. https://doi.org/10.1038/nature07067

Ahmer, B. M., M. Tran, and F. Heffron, 1999 The virulence plasmid of Salmonella typhimurium is self-transmissible. J. Bacteriol. 181: 1364–1368.

Andersen, J. B., C. Sternberg, L. K. Poulsen, S. P. Bjorn, M. Givskov *et al.*, 1998 New unstable variants of green fluorescent protein for studies of transient gene expression in bacteria. Appl. Environ. Microbiol. 64: 2240–2246.

Arnoldini, M., I. A. Vizcarra, R. Pena-Miller, N. Stocker, M. Diard *et al.*, 2014 Bistable expression of virulence genes in *Salmonella* leads to the formation of an antibiotic-tolerant subpopulation. PLoS Biol. 12: e1001928. https://doi.org/10.1371/journal.pbio.1001928

Bäumler, A. J., and V. Sperandio, 2016 Interactions between the microbiota and pathogenic bacteria in the gut. Nature 535: 85–93. https://doi.org/10.1038/nature18849

Brown, N. F., B. A. Vallance, B. K. Coombes, Y. Valdez, B. A. Coburn *et al.*, 2005 *Salmonella* pathogenicity island 2 is expressed prior to penetrating the intestine. PLoS Pathog. 1: e32. https://doi.org/10.1371/journal.ppat.0010032

Browne, S. H., M. L. Lesnick, and D. G. Guiney, 2002 Genetic requirements for *Salmonella*-induced cytopathology in human monocyte-derived macrophages. Infect. Immun. 70: 7126–7135. https://doi.org/10.1128/IAI.70.12.7126-7135.2002

Browne, S. H., P. Hasegawa, S. Okamoto, J. Fierer, and D. G. Guiney, 2008 Identification of *Salmonella* SPI-2 secretion system components required for SpvB-mediated cytotoxicity in macrophages and virulence in mice. FEMS Immunol. Med. Microbiol. 52: 194–201. https://doi.org/10.1111/j.1574-695X.2007.00364.x

Bustamante, V. H., L. C. Martinez, F. J. Santana, L. A. Knodler, O. Steele-Mortimer *et al.*, 2008 HilD-mediated transcriptional cross-talk between SPI-1 and SPI-2. Proc. Natl. Acad. Sci. USA 105: 14591–14596. https://doi.org/10.1073/pnas.0801205105

Camacho, E. M., and J. Casadesus, 2002 Conjugal transfer of the virulence plasmid of *Salmonella enterica* is regulated by the leucine-responsive regulatory protein and DNA adenine methylation. Mol. Microbiol. 44: 1589–1598. https://doi.org/10.1046/j.1365-2958.2002.02981.x

Cano, D. A., M. Martinez-Moya, M. G. Pucciarelli, E. A. Groisman, J. Casadesus *et al.*, 2001 *Salmonella enterica* serovar Typhimurium response involved in attenuation of pathogen intracellular proliferation. Infect. Immun. 69: 6463–6474. https://doi.org/10.1128/IAI.69.10.6463-6474.2001

Cenens, W., M. T. Mebrhatu, A. Makumi, P. J. Ceyssens, R. Lavigne *et al.*, 2013 Expression of a novel P22 ORFan gene reveals the phage carrier state in *Salmonella* Typhimurium. PLoS Genet. 9: e1003269. https://doi.org/10.1371/journal.pgen.1003269

Cherepanov, P. P., and W. Wackernagel, 1995 Gene disruption in *Escherichia coli*: Tc^R and Km^R cassettes with the option of Flp-catalyzed excision of the antibiotic-resistance determinant. Gene 158: 9–14. https://doi.org/10.1016/0378-1119(95)00193-A

Clark, D. J., and O. Maaløe, 1967 DNA replication and the division cycle in *Escherichia coli*. J. Mol. Biol. 23: 99–112. https://doi.org/10.1016/S0022-2836(67)80070-6

Coburn, B., G. A. Grassl, and B. B. Finlay, 2007 *Salmonella*, the host and disease: a brief review. Immunol. Cell Biol. 85: 112–118. https://doi.org/10.1038/sj.icb.7100007

Datsenko, K. A., and B. L. Wanner, 2000 One-step inactivation of chromosomal genes in *Escherichia coli* K-12 using PCR products. Proc. Natl. Acad. Sci. USA 97: 6640–6645. https://doi.org/10.1073/pnas.120163297

Davis, R. W., D. Botstein, and J. R. Roth, 1980 *Advanced Bacterial Genetics*. Cold Spring Harbor Laboratory Press, Cold Spring Harbor, NY.
Deiwick, J., T. Nikolaus, S. Erdogan, and M. Hensel, 1999 Environmental regulation of *Salmonella* pathogenicity island 2 gene expression. Mol. Microbiol. 31: 1759–1773. https://doi.org/10.1046/j.1365-2958.1999.01312.x
Diard, M., V. Garcia, L. Maier, M. N. Remus-Emsermann, R. R. Regoes *et al.*, 2013 Stabilization of cooperative virulence by the expression of an avirulent phenotype. Nature 494: 353–356. https://doi.org/10.1038/nature11913
Eldar, A., and M. B. Elowitz, 2010 Functional roles for noise in genetic circuits. Nature 467: 167–173. https://doi.org/10.1038/nature09326
El-Gedaily, A., G. Paesold, and M. Krause, 1997 Expression profile and subcellular location of the plasmid-encoded virulence (Spv) proteins in wild-type Salmonella dublin. Infect. Immun. 65: 3406–3411.
Fabrega, A., and J. Vila, 2013 *Salmonella enterica* serovar Typhimurium skills to succeed in the host: virulence and regulation. Clin. Microbiol. Rev. 26: 308–341. https://doi.org/10.1128/CMR.00066-12
Fang, F. C., S. J. Libby, N. A. Buchmeier, P. C. Loewen, J. Switala *et al.*, 1992 The alternative sigma factor *katF* (*rpoS*) regulates *Salmonella* virulence. Proc. Natl. Acad. Sci. USA 89: 11978–11982. https://doi.org/10.1073/pnas.89.24.11978
Fass, E., and E. A. Groisman, 2009 Control of *Salmonella* pathogenicity island-2 gene expression. Curr. Opin. Microbiol. 12: 199–204. https://doi.org/10.1016/j.mib.2009.01.004
Ferrell, J. E., Jr., 2002 Self-perpetuating states in signal transduction: positive feedback, double-negative feedback and bistability. Curr. Opin. Cell Biol. 14: 140–148. https://doi.org/10.1016/S0955-0674(02)00314-9
Figueira, R., and D. W. Holden, 2012 Functions of the *Salmonella* pathogenicity island 2 (SPI-2) type III secretion system effectors. Microbiology 158: 1147–1161. https://doi.org/10.1099/mic.0.058115-0
Gotoh, H., N. Okada, Y. G. Kim, K. Shiraishi, N. Hirami *et al.*, 2003 Extracellular secretion of the virulence plasmid-encoded ADP-ribosyltransferase SpvB in *Salmonella*. Microb. Pathog. 34: 227–238. https://doi.org/10.1016/S0882-4010(03)00034-2
Grabe, G. J., Y. Zhang, M. Przydacz, N. Rolhion, Y. Yang *et al.*, 2016 The *Salmonella* effector SpvD is a cysteine hydrolase with a serovar-specific polymorphism influencing catalytic activity, suppression of immune responses, and bacterial virulence. J. Biol. Chem. 291: 25853–25863. https://doi.org/10.1074/jbc.M116.752782
Grob, P., and D. G. Guiney, 1996 In vitro binding of the *Salmonella* Dublin virulence plasmid regulatory protein SpvR to the promoter regions of *spvA* and *spvR*. J. Bacteriol. 178: 1813–1820. https://doi.org/10.1128/jb.178.7.1813-1820.1996
Guilloteau, L. A., T. S. Wallis, A. V. Gautier, S. MacIntyre, D. J. Platt *et al.*, 1996 The *Salmonella* virulence plasmid enhances *Salmonella*-induced lysis of macrophages and influences inflammatory responses. Infect. Immun. 64: 3385–3393.
Guiney, D. G., and J. Fierer, 2011 The role of the *spv* genes in *Salmonella* pathogenesis. Front. Microbiol. 2: 129. https://doi.org/10.3389/fmicb.2011.00129
Gulig, P. A., and T. J. Doyle, 1993 The *Salmonella* Typhimurium virulence plasmid increases the growth rate of salmonellae in mice. Infect. Immun. 61: 504–511.
Haneda, T., Y. Ishii, H. Shimizu, K. Ohshima, N. Iida *et al.*, 2012 *Salmonella* type III effector SpvC, a phosphothreonine lyase, contributes to reduction in inflammatory response during intestinal phase of infection. Cell. Microbiol. 14: 485–499. https://doi.org/10.1111/j.1462-5822.2011.01733.x
Hautefort, I., M. J. Proenca, and J. C. Hinton, 2003 Single-copy green fluorescent protein gene fusions allow accurate measurement of *Salmonella* gene expression in vitro and during infection of mammalian cells. Appl. Environ. Microbiol. 69: 7480–7491. https://doi.org/10.1128/AEM.69.12.7480-7491.2003
Headley, V. L., and S. M. Payne, 1990 Differential protein expression by *Shigella flexneri* in intracellular and extracellular environments. Proc. Natl. Acad. Sci. USA 87: 4179–4183. https://doi.org/10.1073/pnas.87.11.4179
Hébrard, M., C. Kroger, S. K. Sivasankaran, K. Handler, and J. C. Hinton, 2011 The challenge of relating gene expression to the virulence of *Salmonella enterica* serovar Typhimurium. Curr. Opin. Biotechnol. 22: 200–210. https://doi.org/10.1016/j.copbio.2011.02.007
Hensel, M., J. E. Shea, C. Gleeson, M. D. Jones, E. Dalton *et al.*, 1995 Simultaneous identification of bacterial virulence genes by negative selection. Science 269: 400–403. https://doi.org/10.1126/science.7618105
Jarvik, T., C. Smillie, E. A. Groisman, and H. Ochman, 2010 Short-term signatures of evolutionary change in the *Salmonella enterica* serovar Typhimurium 14028 genome. J. Bacteriol. 192: 560–567. https://doi.org/10.1128/JB.01233-09
Kowarz, L., C. Coynault, V. Robbe-Saule, and F. Norel, 1994 The *Salmonella* Typhimurium *katF* (*rpoS*) gene: cloning, nucleotide sequence, and regulation of *spvR* and *spvABCD* virulence plasmid genes. J. Bacteriol. 176: 6852–6860. https://doi.org/10.1128/jb.176.22.6852-6860.1994
Kwon, Y. M., and S. C. Ricke, 2000 Efficient amplification of multiple transposon-flanking sequences. J. Microbiol. Methods 41: 195–199. https://doi.org/10.1016/S0167-7012(00)00159-7
Laughlin, R. C., L. A. Knodler, R. Barhoumi, H. R. Payne, J. Wu *et al.*, 2014 Spatial segregation of virulence gene expression during acute enteric infection with *Salmonella enterica* serovar Typhimurium. MBio 5: e00946–13. https://doi.org/10.1128/mBio.00946-13
Lee, C. A., B. D. Jones, and S. Falkow, 1992 Identification of a *Salmonella* Typhimurium invasion locus by selection for hyperinvasive mutants. Proc. Natl. Acad. Sci. USA 89: 1847–1851. https://doi.org/10.1073/pnas.89.5.1847
Libby, S. J., L. G. Adams, T. A. Ficht, C. Allen, H. A. Whitford *et al.*, 1997 The *spv* genes on the *Salmonella* Dublin virulence plasmid are required for severe enteritis and systemic infection in the natural host. Infect. Immun. 65: 1786–1792.
Libby, S. J., M. Lesnick, P. Hasegawa, E. Weidenhammer, and D. G. Guiney, 2000 The *Salmonella* virulence plasmid *spv* genes are required for cytopathology in human monocyte-derived macrophages. Cell. Microbiol. 2: 49–58. https://doi.org/10.1046/j.1462-5822.2000.00030.x
Lutz, R., and H. Bujard, 1997 Independent and tight regulation of transcriptional units in *Escherichia coli* via the LacR/O, the TetR/O and AraC/I1–I2 regulatory elements. Nucleic Acids Res. 25: 1203–1210. https://doi.org/10.1093/nar/25.6.1203
MacKenzie, K. D., Y. Wang, D. J. Shivak, C. S. Wong, L. J. Hoffman *et al.*, 2015 Bistable expression of CsgD in *Salmonella enterica* serovar Typhimurium connects virulence to persistence. Infect. Immun. 83: 2312–2326. https://doi.org/10.1128/IAI.00137-15
Mangan, M. W., S. Lucchini, V. Danino, T. O. Croinin, J. C. Hinton *et al.*, 2006 The integration host factor (IHF) integrates stationary-phase and virulence gene expression in *Salmonella enterica* serovar Typhimurium. Mol. Microbiol. 59: 1831–1847. https://doi.org/10.1111/j.1365-2958.2006.05062.x
Marshall, D. G., B. J. Sheehan, and C. J. Dorman, 1999 A role for the leucine-responsive regulatory protein and integration host factor in the regulation of the *Salmonella* plasmid virulence (spv) locus in *Salmonella* Typhimurium. Mol. Microbiol. 34: 134–145. https://doi.org/10.1046/j.1365-2958.1999.01587.x
Martínez-García, E., B. Calles, M. Arevalo-Rodriguez, and V. de Lorenzo, 2011 pBAM1: an all-synthetic genetic tool for analysis and construction of complex bacterial phenotypes. BMC Microbiol. 11: 38. https://doi.org/10.1186/1471-2180-11-38
Martins, B. M., and J. C. Locke, 2015 Microbial individuality: how single-cell heterogeneity enables population level strategies. Curr. Opin. Microbiol. 24: 104–112. https://doi.org/10.1016/j.mib.2015.01.003

Mazurkiewicz, P., J. Thomas, J. A. Thompson, M. Liu, L. Arbibe *et al.*, 2008 SpvC is a *Salmonella* effector with phosphothreonine lyase activity on host mitogen-activated protein kinases. Mol. Microbiol. 67: 1371–1383. https://doi.org/10.1111/j.1365-2958.2008.06134.x

McQuiston, J. R., S. Herrera-Leon, B. C. Wertheim, J. Doyle, P. I. Fields *et al.*, 2008 Molecular phylogeny of the salmonellae: relationships among *Salmonella* species and subspecies determined from four housekeeping genes and evidence of lateral gene transfer events. J. Bacteriol. 190: 7060–7067. https://doi.org/10.1128/JB.01552-07

Mills, D. M., V. Bajaj, and C. A. Lee, 1995 A 40 kb chromosomal fragment encoding *Salmonella* Typhimurium invasion genes is absent from the corresponding region of the *Escherichia coli* K-12 chromosome. Mol. Microbiol. 15: 749–759. https://doi.org/10.1111/j.1365-2958.1995.tb02382.x

Morgan, E., 2007 *Salmonella Pathogenicity Islands*. Horizon bioscience, Wymondham, United Kingdom.

Norel, F., V. Robbe-Saule, M. Y. Popoff, and C. Coynault, 1992 The putative sigma factor KatF (RpoS) is required for the transcription of the *Salmonella* Typhimurium virulence gene *spvB* in *Escherichia coli*. FEMS Microbiol. Lett. 78: 271–276. https://doi.org/10.1111/j.1574-6968.1992.tb05580.x

O'Byrne, C. P., and C. J. Dorman, 1994a The spv virulence operon of *Salmonella* Typhimurium LT2 is regulated negatively by the cyclic AMP (cAMP)-cAMP receptor protein system. J. Bacteriol. 176: 905–912. https://doi.org/10.1128/jb.176.3.905-912.1994

O'Byrne, C. P., and C. J. Dorman, 1994b Transcription of the *Salmonella* Typhimurium spv virulence locus is regulated negatively by the nucleoid-associated protein H-NS. FEMS Microbiol. Lett. 121: 99–105. https://doi.org/10.1111/j.1574-6968.1994.tb07082.x

Ochman, H., F. C. Soncini, F. Solomon, and E. A. Groisman, 1996 Identification of a pathogenicity island required for *Salmonella* survival in host cells. Proc. Natl. Acad. Sci. USA 93: 7800–7804. https://doi.org/10.1073/pnas.93.15.7800

Otto, H., D. Tezcan-Merdol, R. Girisch, F. Haag, M. Rhen *et al.*, 2000 The spvB gene-product of the *Salmonella enterica* virulence plasmid is a mono(ADP-ribosyl)transferase. Mol. Microbiol. 37: 1106–1115. https://doi.org/10.1046/j.1365-2958.2000.02064.x

Phoebe Lostroh, C., and C. A. Lee, 2001 The *Salmonella* pathogenicity island-1 type III secretion system. Microbes Infect. 3: 1281–1291. https://doi.org/10.1016/S1286-4579(01)01488-5

Rhen, M., and C. J. Dorman, 2005 Hierarchical gene regulators adapt *Salmonella enterica* to its host milieus. Int. J. Med. Microbiol. 294: 487–502. https://doi.org/10.1016/j.ijmm.2004.11.004

Robbe-Saule, V., F. Schaeffer, L. Kowarz, and F. Norel, 1997 Relationships between H-NS, sigma S, SpvR and growth phase in the control of *spvR*, the regulatory gene of the *Salmonella* plasmid virulence operon. Mol. Gen. Genet. 256: 333–347. https://doi.org/10.1007/s004380050577

Robbe-Saule, V., L. Kowarz, and F. Norel, 1999 A coding segment of the virulence regulatory gene *spvR* enhances expression of *spvR-lacZ* and *spvR-gfp* translational fusions in *Salmonella* Typhimurium. Mol. Gen. Genet. 261: 472–479. https://doi.org/10.1007/s004380050990

Rolhion, N., R. C. Furniss, G. Grabe, A. Ryan, M. Liu *et al.*, 2016 Inhibition of nuclear transport of NF-κB p65 by the *Salmonella* type III secretion system effector SpvD. PLoS Pathog. 12: e1005653. https://doi.org/10.1371/journal.ppat.1005653

Rotger, R., and J. Casadesus, 1999 The virulence plasmids of *Salmonella*. Int. Microbiol. 2: 177–184.

Roudier, C., J. Fierer, and D. G. Guiney, 1992 Characterization of translation termination mutations in the *spv* operon of the *Salmonella* virulence plasmid pSDL2. J. Bacteriol. 174: 6418–6423. https://doi.org/10.1128/jb.174.20.6418-6423.1992

Saini, S., J. R. Ellermeier, J. M. Slauch, and C. V. Rao, 2010 The role of coupled positive feedback in the expression of the SPI1 type three secretion system in *Salmonella*. PLoS Pathog. 6: e1001025. https://doi.org/10.1371/journal.ppat.1001025

Sambrook, J., and R. W. Russell, 2001 *Molecular Cloning: A Laboratory Manual*. Cold Spring Harbor Laboratory Press, Cold Spring Harbor, NY.

Schmieger, H., 1972 Phage P22-mutants with increased or decreased transduction abilities. Mol. Gen. Genet. 119: 75–88. https://doi.org/10.1007/BF00270447

Sheehan, B. J., and C. J. Dorman, 1998 In vivo analysis of the interactions of the LysR-like regulator SpvR with the operator sequences of the *spvA* and *spvR* virulence genes of *Salmonella* Typhimurium. Mol. Microbiol. 30: 91–105. https://doi.org/10.1046/j.1365-2958.1998.01041.x

Sliusarenko, O., J. Heinritz, T. Emonet, and C. Jacobs-Wagner, 2011 High-throughput, subpixel precision analysis of bacterial morphogenesis and intracellular spatio-temporal dynamics. Mol. Microbiol. 80: 612–627. https://doi.org/10.1111/j.1365-2958.2011.07579.x

Spink, J. M., G. D. Pullinger, M. W. Wood, and A. J. Lax, 1994 Regulation of *spvR*, the positive regulatory gene of *Salmonella* plasmid virulence genes. FEMS Microbiol. Lett. 116: 113–121. https://doi.org/10.1111/j.1574-6968.1994.tb06684.x

Sterzenbach, T., R. W. Crawford, S. E. Winter, and A. J. Baümler, 2013 *Salmonella Virulence Mechanisms and their Genetic Basis*, Chap 5. CAB International, Wallingford, United Kingdom. https://doi.org/10.1079/9781845939021.0080

Stewart, M. K., and B. T. Cookson, 2012 Non-genetic diversity shapes infectious capacity and host resistance. Trends Microbiol. 20: 461–466. https://doi.org/10.1016/j.tim.2012.07.003

Sturm, A., M. Heinemann, M. Arnoldini, A. Benecke, M. Ackermann *et al.*, 2011 The cost of virulence: retarded growth of *Salmonella* Typhimurium cells expressing type III secretion system 1. PLoS Pathog. 7: e1002143. https://doi.org/10.1371/journal.ppat.1002143

Süel, G. M., J. Garcia-Ojalvo, L. M. Liberman, and M. B. Elowitz, 2006 An excitable gene regulatory circuit induces transient cellular differentiation. Nature 440: 545–550. https://doi.org/10.1038/nature04588

Tezcan-Merdol, D., L. Engstrand, and M. Rhen, 2005 *Salmonella* enterica SpvB-mediated ADP-ribosylation as an activator for host cell actin degradation. Int. J. Med. Microbiol. 295: 201–212. https://doi.org/10.1016/j.ijmm.2005.04.008

Valone, S. E., and G. K. Chikami, 1991 Characterization of three proteins expressed from the virulence region of plasmid pSDL2 in *Salmonella* Dublin. Infect. Immun. 59: 3511–3517.

Wilmes-Riesenberg, M. R., J. W. Foster, and R. Curtiss, III, 1997 An altered *rpoS* allele contributes to the avirulence of *Salmonella* Typhimurium LT2. Infect. Immun. 65: 203–210.

Wilson, J. A., and P. A. Gulig, 1998 Regulation of the *spvR* gene of the *Salmonella* Typhimurium virulence plasmid during exponential-phase growth in intracellular salts medium and at stationary phase in L broth. Microbiology 144: 1823–1833. https://doi.org/10.1099/00221287-144-7-1823

Wilson, J. A., T. J. Doyle, and P. A. Gulig, 1997 Exponential-phase expression of spvA of the *Salmonella* Typhimurium virulence plasmid: induction in intracellular salts medium and intracellularly in mice and cultured mammalian cells. Microbiology 143: 3827–3839. https://doi.org/10.1099/00221287-143-12-3827

Wilson, K., 2001 *Preparation of Genomic DNA From Bacteria in Current Protocols in Molecular Biology*. John Wiley & Sons, Inc., New York.

Worley, M. J., K. H. Ching, and F. Heffron, 2000 *Salmonella* SsrB activates a global regulon of horizontally acquired genes. Mol. Microbiol. 36: 749–761. https://doi.org/10.1046/j.1365-2958.2000.01902.x

Young, J. W., J. C. Locke, and M. B. Elowitz, 2013 Rate of environmental change determines stress response specificity. Proc. Natl. Acad. Sci. USA 110: 4140–4145. https://doi.org/10.1073/pnas.1213060110

Communicating editor: J. Lawrence